Biosensors and Bioelectronics 55 (2014) 26–31

Contents lists available at ScienceDirect

Biosensors and Bioelectronics

journal homepage: www.elsevier.com/locate/bios

Coiled-coil peptide based sensor for ultra-sensitive thrombin detection

Patthara Kongsuphol, Sunil K. Arya *, Chee Chung Wong, Lee Joseph Polla, Mi Kyoung Park

Institute of Microelectronics, 11 Science Park Road, Singapore Science Park II, 117685 Singapore, Singapore

ARTICLE INFO

Article history:
Received 17 September 2013
Received in revised form
15 November 2013
Accepted 25 November 2013
Available online 4 December 2013

Keywords:
Coiled-coil peptide
Thrombin
Biosensor
Electrochemical impedance
Self-assembled monolayer

ABSTRACT

Comb structured gold microelectrode array (CSGMA) functionalized with self-assembled monolayer of thiol terminated coiled-coil peptide (CCP) linked together by the thrombin specific cleavage site (Leu–Val–Pro–Arg–Gly–Ser) has been used to fabricate an ultrasensitive, disposable, electrochemical thrombin biosensor. CCP with thiol at one end provides the ease of CSGMA functionalization and the presence of thrombin specific peptide in the middle of coiled-coil peptide provides site for thrombin capture and detection. CCP/CSGMA electrodes were characterized using label-free electrochemical impedance (EIS) technique and exposed to solutions with different thrombin concentrations for its estimation. Results reveal that CCP/CSGMA electrodes have a limit of detection (LOD) of 10 fg/ml (28 fM) and are able to detect catalytic activity of thrombin within 30 min time frame. CCP/CSGMA electrodes were found to be selective against other IgG anti-bodies such as DO1 and HA. Thus, CCP/CSGMA electrodes provide high specificity toward thrombin detection and mechanistic details of binding and cleavage process.

1. Introduction

Thrombin, a serine protease, plays an important role in blood coagulation process via two opposite functions, a procoagulant factor and an anticoagulant factor. For its role as a procoagulant factor, thrombin converts a soluble fibrinogen to an insoluble fibrin clot that anchors platelet to the injured tissue sites and initiates tissue repair process. On the other hand, thrombin acts as an anticoagulant factor when it binds to thrombomodulin. Binding of thrombin to thrombomodulin activates protein C and initiates anticoagulation process (Cera and Gruber, 2009). In addition to its role in blood coagulation process, thrombin involves in onset and progression of several diseases (Borissoff et al., 2009; Kobrinsky and Karpatkin, 2009). Thrombin is a key factor for the development of atherosclerosis and its acute vascular complications (Borissoff et al., 2009). At the early stage of atherosclerotic plaque formation, thrombin is a critical mediator of coagulation, inflammation, and vessel wall crosstalk. Also at the advance stage, thrombin plays a major role in platelet-mediated pro-inflammatory cascades that contribute to plaque progression, vessel wall destabilization and rupture (Borissoff et al., 2009). Further, thrombin also involves in angiogenesis process (Tsopanoglou and Maragoudakis, 2009), which promotes progression of several diseases including cancer (Arnold, 1985; Polverini, 1995). Keeping clinical importance of thrombin in mind, establishment of fast and reliable thrombin detection technique would be of tremendous value.

The common techniques in use to detect the presence/activity of thrombin include the detection of the thrombin downstream effectors (Shainoff et al., 1960) and the enzyme-linked immunosorbent assay (ELISA). The former is an indirect method of thrombin detection whereas the latter is a direct method that gives good quality data. Although ELISA gives good quality data, it is a time-consuming process, requires labeling, and restricts only to matched pair of monoclonal antibodies.

Electrochemical immunosensors especially electrochemical impedance spectroscopy (EIS) based label free sensing have recently gain much attention as a means for the detection of desired proteins, immunoglobin, biomarkers and biological toxins in various food, environment, and clinical diagnostics situations (Akter et al., 2013; Arya et al., 2010; Chen et al., 2010; Conzuelo et al., 2013; Dong et al., 2013; Elshafey et al., 2013; Kaushik et al., 2013; Montrose et al., 2013; Pui et al., 2013; Elyasi et al., 2013; Shahmiri et al., 2013; Moradi et al., 2013; Karimi-Maleh et al., 2013). EIS is a very powerful non-destructive method that can be employed to measure biological interactions and analyze interfacial properties related to bio-recognition events occurring at the modified surfaces.

Many EIS-based thrombin biosensors have been developed to bypass ELISA disadvantages, shorten the detection times, and improve specificity and sensitivity (Table 1). Most of the EIS-based thrombin biosensors utilized the known sequence of thrombin aptamer (Latham et al., 1994) as probes to detect thrombin (Li et al., 2011; Xu et al., 2013; Wang et al., 2012; Evtugyn et al., 2013; Jiang et al., 2014). Aptamers are oligonucleotide that selectively bind proteins or target molecules with high affinity. EIS technique provides short incubation time and

* Corresponding author. Tel.: +65 67705621; fax: +65 64640517.
E-mail address: sunilarya333@gmail.com (S.K. Arya).

0956-5663/$ - see front matter © 2013 Elsevier B.V. All rights reserved.
http://dx.doi.org/10.1016/j.bios.2013.11.070

Table 1
Comparison of different thrombin biosensors.

Technique	Probe unit	Detection time	LOD	Catalytic activity	Ref.
Colorimetric assay	Fib–Au NPs[d]	1.5 h	40 fM	Y	Chen et al. (2010)
Colorimetric assay	Au NPs[c]	25 min	70 pM	Y	Chen et al. (2011)
Colorimetric assay	Fib–Au NPs[d]	0.5–8 h	3.2 fM at 8 h and 420 fM at 0.5 h	Y	Niu et al. (2013)
Surface-enhanced Raman scattering	Apt–Au Nps[e]	3 h	20 pM	N	Hu et al. (2009)
Chemiluminescence (sandwich assay based on ELISA principle)	$ZnPc(OAr)_4$@SiO2[f] labeled aptamer antibody	N/A	80 pM	N	Jiang et al. (2014)
EIS[a]	Apt–Au Nps[e]	N/A	13 pM	N	Li et al. (2011)
EIS[a]	Aptamer film	40 min	4.7 pM	N	Xu et al. (2013)
EIS[a]	Aptamer graphine	20 min	0.45 fM	N	Wang et al. (2012)
EIS[a], CV[b]	Apt–ZnO nanorod[g]	20 min	10 pM	N	Evtugyn et al. (2013)
EIS[a]	Coiled-coil peptide	10–30 min	28 fM	Y	The present study

[a] Electrochemical impedance spectroscopy.
[b] Cyclic boltammetry.
[c] Gold nanoparticles.
[d] Fibrinogen–gold nanoparticles.
[e] Aptamer–gold nanoparticles.
[f] Tetra-α-(2, 4-di-tert-butylphenoxy)-phthalocyaninato zinc encapsulated in silica nanoparticles.
[g] Aptamer–zinc oxide nanorod.

real-time data monitoring, however, since the DNA-aptamer probes cannot be cleaved by thrombin, it cannot determine thrombin catalytic activity. Recently, colorimetric detection of thrombin using a gold nanoparticle-based technique has been reported (Chen et al., 2010; Niu et al., 2013). This method is able to detect both the presence and catalytic activity of thrombin, however, the incubation and detection time could take as long as several hours (Chen et al., 2010; Niu et al., 2013).

Heterodimerization of coiled-coil peptide (CCP) has been described as a powerful alternative tool for biosensor development (Chao et al., 1998). The important feature of CCP lies within its two non-covalently assembled helical peptide building blocks, in which one of the coil can be modified with thiol terminal for easy surface functionalization and the other coil can be fused with protein of particular interest. Studies have shown that CCPs are both structurally and kinetically stable in solution at neutral pH (Chao et al., 1998). Coiled-coil protein can be synthesized in vitro (McClain et al., 2001) thus, allowing production of large quantities at relatively low cost with long storage life. CCP has advantage over aptamer in a way that it is a protein, which can be used to detect protein activity (e.g., enzyme, receptor, etc.), and has advantage over antibodies in term of lower production cost and better stability. Altogether, the unique structure, the chemical resistance properties, and the lower production cost of CCP make it a powerful tool for development of biosensors.

In the present work, we have developed a novel label free coiled-coil peptide (CCP) based thrombin biosensor, which has high specificity and sensitivity toward thrombin. The thiol terminated CCP is linked together by the thrombin specific cleavage site (Leu–Val–Pro–Arg–Gly–Ser). Coiled-coil peptide with thiol at one end provides the ease of gold electrode surface functionalization and the presence of thrombin specific peptide in the middle of the CCP provides site for thrombin capture and detection. In presence of thrombin, thrombin bind to CCP and at the critical concentration, cleave its specific binding site, releasing one coil of peptide out of its pair. This biosensor could detect both the presence and catalytic activity of thrombin within 30 min period. This approach provides high specificity toward thrombin detection and provides the mechanistic details of binding and cleavage process.

2. Materials and methods

2.1. Chemicals and reagents

Coiled-coil peptide with N-terminus to C-terminus sequence (EKKLAQLEWENQALEKELAQGG-*LVPRGS*-GGAQLKKKLQANKKE-LAQLKWK-CH2-CH2-SH) was procured from Biosynthesis, Inc. Thrombin from human plasma (2949 NIH units/mg) and dimethylsulfoxide (DMSO) was purchased from Sigma. Phosphate buffer solution (PBS, pH = 7.4) was bought from Invitrogen, USA. All other chemicals were of analytical grade and used without purification. Working solutions of thrombin were freshly prepared prior the experiments by diluting with PBS. Stock solution of CCP (1 mg/ml) was prepared in DMSO and stored at −20 °C till use.

2.2. Measurement and apparatus

Electrochemical impedance (EIS) was utilized to characterize the CCP/CSGMA electrodes and to estimate thrombin concentration. EIS measurements were carried out in the frequency range of 0.5 Hz–500 KHz with a 25 mV amplitude using Autolab Potentiostat/Galvanostat (Eco Chemie, Netherlands). EIS measurements were carried out at room temperature using 60 μl PBS solution (10 mM, pH 7.4) containing a mixture of 5 mM $Fe(CN)_6^{4-}$ (Ferrocyanide) and 5 mM of $Fe(CN)_6^{3-}$ (Ferricyanide) i.e., 5 mM $Fe(CN)_6^{3-/4-}$ as a redox probe.

2.3. Gold electrode and CCP/CSGMA electrodes fabrication

CSGMA electrodes were fabricated on oxidized silicon wafer using standard micro-fabrication techniques as described in an earlier report (Arya et al., 2013). For CSGMA electrodes 5 μm wide and 3200 μm long electrode bands with 15 μm spacing, distributed over 5500 μm length were fabricated and utilized.

The fabricated electrodes were pre-cleaned with acetone, ethanol and with copious amounts of de-ionized water followed by cleaning with UV-ozone for 20 min. For CCP self-assembled monolayer (SAM) formation 50 μl of CCP stock solution was diluted in 5 ml of PBS to get 10 μg/ml working solution and kept

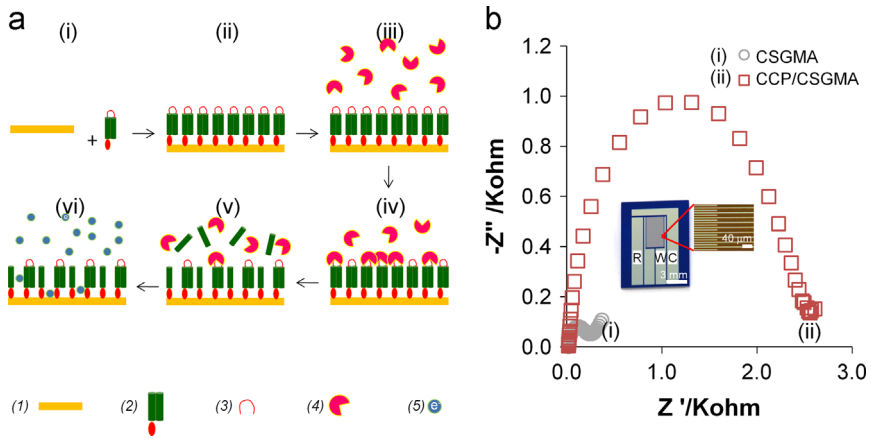

Fig. 1. Biosensor development and verification. (a) Scheme represents CCP SAM formation and thrombin detection mechanism. Symbols represent (1) gold electrode, (2) thiol-terminated CCP, (3) thrombin specific cleavage site, (4) thrombin, and (5) redox molecule. (i) Thiol-terminated CCP containing thrombin specific cleavage site is (ii) immobilized onto gold electrode surface. (iii) Upon the present of thrombin, (iv) thrombin will bind to and subsequently and (v) cleave its specific cleavage site, releasing one coil peptide out of its pair. (vi) The biosensor is then washed several times with PBS and incubated with redox probe (10 mM PBS pH 7.4 containing 5 mM $Fe(CN)_6^{3-/4-}$) for 1 min. and finally undergoes EIS spectra recording. (b) Nyquist plots of (i) *CSGMA* electrode, (ii) *CCP/CSGMA* electrode. Inset shows the optical image of CSGMA electrode chip (R: reference; W: working and C: counter electrode).

at room temperature for 10 min for protein refolding. CSGMA electrodes were then immersed in CCP working solution and left overnight for SAM formation. CCP SAM modified electrodes were rinsed with PBS to remove any unbound CCP and stored in PBS at 4 °C till used.

3. Results and discussion

3.1. CCP/CSGMA electrode fabrication

Fig. 1a shows the schematic of CCP/CSGMA electrode fabrication with thrombin detection mechanism. CCP SAM formation via thiol–gold interaction results in the exposure of thrombin specific peptide on the upper surface of electrode. Upon incubation with thrombin, peptide starts binding with thrombin and at critical concentration, the cleavage of peptide starts, which causes removal of free strand of CCP into the solution. Fig. 1b shows the nyquist plots of EIS spectra for blank CSGMA and after CCP SAM formation. In the nyquist plot (Fig. 1b), the increase in diameter of semicircle i.e., R_{ct}, confirm the SAM formation and is attributed to the presence of CCP molecules, which result in decrease of the charge transfer from solution to electrode surface due to their non conducting nature.

3.2. Time and concentration dependent EIS studies

The CCP/CSGMA electrode was utilized to study the interaction between immobilized thrombin specific peptide and thrombin concentrations. For each concentration, the CCP/CSGMA electrode was incubated in thrombin solution for desired period, followed by PBS washing and EIS spectra recording using PBS (10 mM, pH 7.4) containing 5 mM $Fe(CN)_6^{3-/4-}$ as a redox probe. All experiments were conducted under consistent parameters at room temperature. Fig. 2a–c shows nyquist spectra of 100 fg/ml, 1 pg/ml, and 10 pg/ml thrombin at different times of incubation in which observed changes in R_{ct} (the diameter of the Nyquist plots) supports our suggested mechanism (Fig. 1). From Fig. 2a, it is clear that R_{ct} for thrombin concentration lower than critical concentration increases with increasing incubation time over 30 min time frame. The increase in R_{ct} is attributed to the binding of thrombin to the immobilized CCP on the CSGMA, producing an insulating layer that decreases the charge transfer for the redox probe. On the other hand in Fig. 2b and c, R_{ct} for thrombin concentration larger than critical concentration increases with increasing incubation time up to 10 min and when critical units of thrombin get accumulated on CCP, it starts cleaving the thrombin specific peptide resulting in release of free peptide chains. Such removal of peptide from surface along with attached thrombin create spaces in surface bound SAM, which thus enhances the charge transfer for the redox probe from solution to electrode surface causing decrease in R_{ct} value. The effect of peptide cleavage can be clearly observed at high thrombin concentration (10 pg/ml, Fig. 2c). Further, from Fig. 2c and b, it is clear that the saturation of surface with thrombin occurs at faster rate for 10 pg/ml concentration as only small increase in R_{ct} was observed after 5 min and decrease in R_{ct} become visible after 10 min and starts going down further than R_{ct} observed for CCP/CSGMA electrode.

Fig. 3a and b shows the normalized R_{ct} [$R_{ct(Tx)}/R_{ct(To)}$] values for different thrombin concentrations and their time responses. Error bar shows the variation from at least triplicate set of experiments. Fig. 3a shows that up to 100 fg/ml, thrombin undergoes simple binding with peptide and no cleavage of peptide occurs. Thus, within 30 min incubation of thrombin up to 100 fg/ml, critical concentration is not reached and the increase in R_{ct} is observed as a function of peptide concentration. Fig. 3b proves the other part of suggested mechanism, where with increasing concentration of thrombin, R_{ct} initially increases and upon reaching the critical concentration, R_{ct} starts decreasing via peptide cleavage over 30 min time frame of incubation. From Fig. 3b, it is clear that critical concentration reaches at 1 pg/ml after 10 min of incubation. Extending incubation of thrombin causes two opposite events, increase in R_{ct} due to increase thrombin binding and decrease in R_{ct} due to peptide cleavage. Thus, the R_{ct} values obtained after 10 min incubation of 1 pg/ml thrombin are the result of thrombin binding and peptide cleavage equilibrium. Further, from Fig. 3b, increase in thrombin concentration beyond 1 pg/ml lead to faster rate of thrombin binding to the peptide thus, the critical concentration reaches even before 10 min and R_{ct} starts to decrease. Altogether, this validates our suggested mechanism of thrombin detection and peptide cleavage activity.

Fig. 4a shows the normalized R_{ct} data for different concentrations of thrombin (10 fg/ml–10 pg/ml) after 10 min of incubation. The data suggests that during the first 10 min of incubation, the sensor can be used to estimate thrombin concentration in the range of 10 fg/ml–1 pg/ml following the logarithmic relation

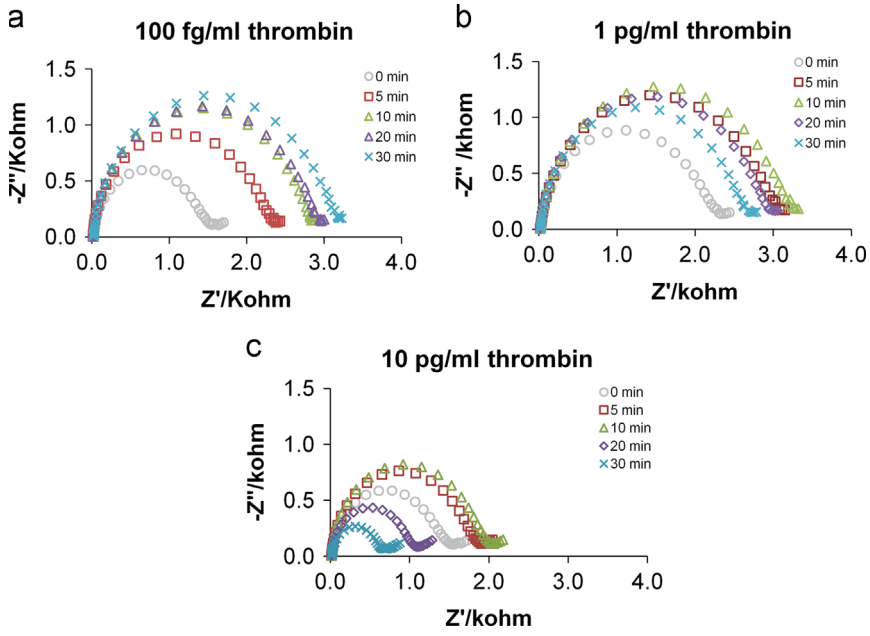

Fig. 2. Nyquist plot of CCP/CSGMA electrode as a function of 100 fg/ml (a) 1 pg/ml (b) and 10 pg/ml (c) thrombin at different incubation times.

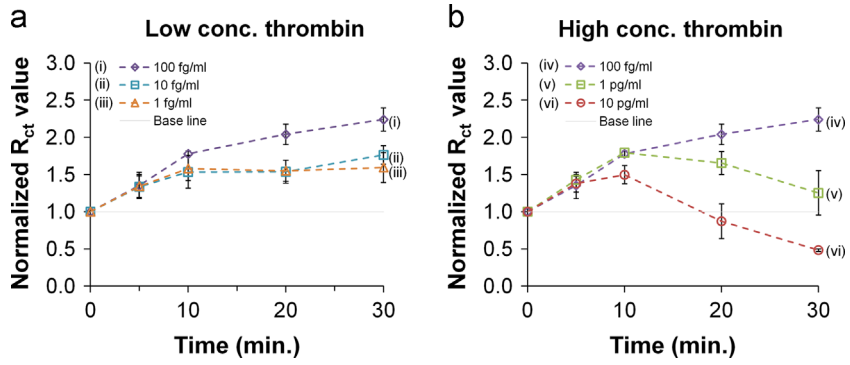

Fig. 3. Different thrombin concentrations and their time responses. (a) Normalized R_{ct} data of different thrombin concentrations ranging from 1 fg/ml to 100 fg/ml and (b) 100 fg/ml to 10 pg/ml at different incubation times (5–30 min).

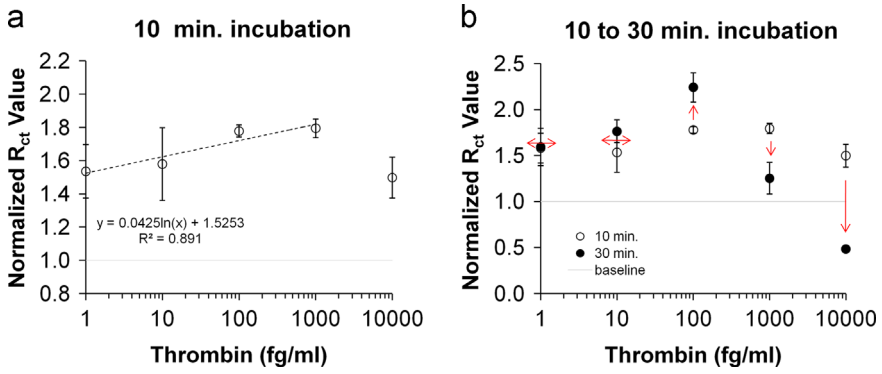

Fig. 4. Different thrombin concentrations and their time responses. (a) Normalized R_{ct} data of different thrombin concentrations (1 fg/ml–10 pg/ml) at 10 min incubation and (b) 10 and 30 min incubation. Arrow indicates shift in R_{ct} value at 30 min as compare to 10 min of incubation (↔ denotes no change, ↑ denotes increase, and ↓ denotes decrease).

"$y = 0.425 \log(x) + 1.5253$", whereas the concentration above 1 pg/ml shows decrease in R_{ct} value after certain time of incubation and do not fit in the logarithmic relation. For higher thrombin concentration, Fig. 4a suggests that the R_{ct} value falls within the same range as the low thrombin concentration (e.g., 10 fg/ml and 10 pg/ml), thus, R_{ct} value of the second time point is required to confirm the actual thrombin concentration. Fig. 4b shows the normalized R_{ct} data for different concentration of thrombin at 10 and 30 min. of incubation. The data shows that at 10 fg/ml, thrombin is saturated after 10 min of incubation and R_{ct} value shows no significant change at 30 min of incubation, whereas at 100 fg/ml, thrombin binding to the peptide does not saturate at 10 min of incubation and the binding increase up to 30 min. of incubation, thus increasing the R_{ct} value. On the other hand, at the concentration

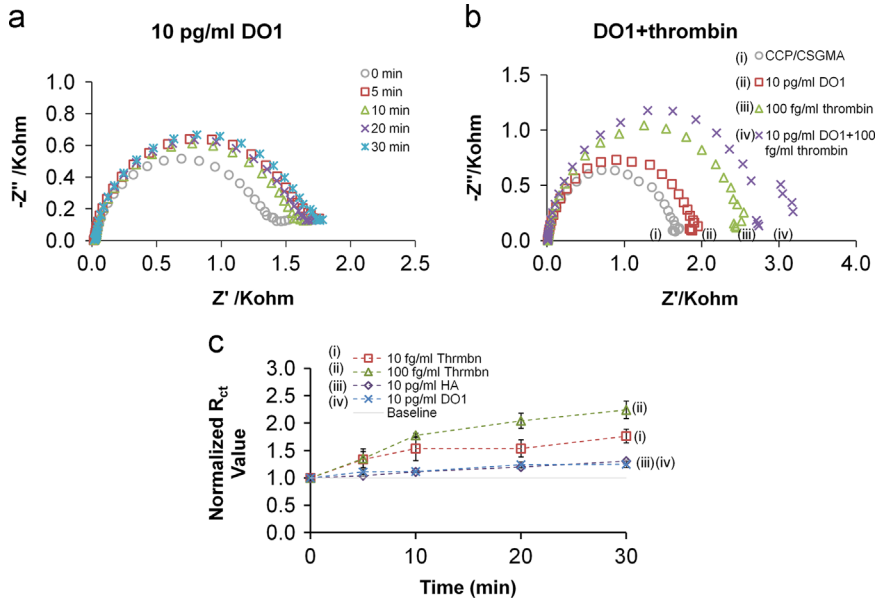

Fig. 5. Selectivity studies of CCP/CSGMA electrode. (a) Nyquist plot of CCP/CSGMA electrode against 10 pg/ml p-53 antibody (clone DO1) at different time of incubation. (b) Nyquist plot of (i) CCP/CSGMA, (ii) 10 pg/ml p-53 antibody (clone DO1), (iii) 100 fg/ml thrombin, and (iv) 10 pg/ml p-53 antibody (clone DO1)+100 fg/ml thrombin at 10 min of incubation. (c) Normalized R_{ct} data at different time of incubation of (i) 10 fg/ml thrombin, (ii) 100 fg/ml thrombin, (iii) 10 pg/ml hemagglutinin (HA) anti-body, and (iv) 10 pg/ml p-53 antibody (clone DO1).

of 1 pg/ml and 10 pg/ml, thrombin starts cleaving the target peptide over 30 min time frame and release out one peptide coil of CCP, therefore lowering the R_{ct} value. Thus, increase or decrease of R_{ct} values at 30 min as compared to 10 min confirms whether the measured thrombin belongs to lower or the higher range of concentration. Further, from Fig. 4b, 30 min of incubation at regular interval can be used to study the mechanism and interaction behavior of thrombin with surface bound peptide.

3.3. Selectivity study of CCP/CSGMA electrode

Selectivity tests were conducted using the CCP/CSGMA electrode against p-53 antibody (clone DO1) and hemagglutinin (HA) anti-body solutions. Fig. 5a shows nquist plots of DO1 incubation over 30 min time frame. It is clear from Fig. 5a that CCP/CSGMA electrode show only a small shift in initial 5 min and thereafter does not show significant change, suggesting minor non specific adsorption on the blank areas of the chip. However, from Fig. 5b, nyquist plots of CCP/CSGMA electrode with (ii) DO1, (iii) thrombin, and (iv) DO1-thrombin mixture, it is clear that the chip preferentially bind to thrombin as high signal is observed at 100 fg/ml when compare to DO1 at 10 pg/ml. Further, signal observed for mixture of thrombin and DO1 confirm the biosensor specificity. Slightly higher value of R_{ct} observed in DO1-thrombin mixture may be attributed to the nonspecific binding of DO1. Altogether, these results suggest that the biosensor preferentially binds to thrombin over DO1. Further Fig. 5c shows the normalized R_{ct} data for DO1 antibody (10 pg/ml), HA antibody (10 pg/ml), thrombin (10 fg/ml) and thrombin (100 fg/ml) over 30 min time frame. From Fig. 5c, it is clear that thrombin even at 10 fg/ml can be distinguished from other even at 5 min.

4. Conclusions

In summary, a comb structured gold microelectrode array functionalized with self-assembled monolayer of thiol terminated coiled-coil peptide linked together by the thrombin specific cleavage site (Leu–Val–Pro–Arg–Gly–Ser) may be used to fabricate an ultrasensitive, disposable, electrochemical thrombin biosensor. Use of CCP with thrombin cleavage site provides the opportunity to detect thrombin linearly from 10 fg/ml to 1pg/ml concentration range within 10 min of incubation and to understand the catalytic activity mechanism of thrombin within 30 min of incubation. CCP/CSGMA electrode shows detection limit of 10 fg/ml (27 fM) and found to be selective against DO1 and HA antibodies. Thus, use of CCP may provide new biosensor platform by replacing antibodies/aptamer as sensing molecule for detection of desired biomolecule.

Acknowledgment

This work was supported by the A*STAR (Agency for Science, Technology and Research), Singapore and JCO Grant number 12302FG015 and IME/12-510041.

References

Akter, R., Kyun, C., Rahman, A., 2013. Bios. Bioelectron. 50, 118–124.
Arnold, F., 1985. Ann. R. Collage Surgeins Engl. 67, 295–298.
Arya, S.K., Chornokur, G., Bhansali, S., 2010. Analyst 135, 1941–1946.
Arya, S.K., Pui, T.S., Wong, C.C., Kumar, S., Rahman, A.R.A., 2013. Langmuir 29, 6770–6777.
Borissoff, J.I., Spronk, H.M.H., Heeneman, S., ten Cate, H., 2009. Cardiovasc. Res. 82, 392–403.
Cera, E.Di, Gruber, A., 2009. In: Maragoudakis, M.E., Sopanoglou, N.E. (Eds.), Thrombin: Physiology and Disease. Springer, New York, pp. 1–18.
Chao, H., Bautista, D.L., Litowski, J., Irvin, R.T., Hodges, R.S., 1998. J. Chromatogr. 715, 307–329.
Chen, C.-K., Huang, C.-C., Chang, H.-T., 2010. Biosens. Bioelectron. 25, 1922–1927.
Chen, Y.-Y., Tseng, C.-W., Chang, H.-Y., Hung, Y.-L., Huan, C.-C., 2011. Biosens. Bioelectron. 26, 3160–3166.
Conzuelo, F., Campuzano, S., Gamella, M., Pinacho, D.G., Reviejo, A.J., Marco, M.P., Pingarrón, J.M., 2013. Biosens. Bioelectron. 50, 100–105.
Dong, J., Zhao, H., Xu, M., Ma, Q., Ai, S., 2013. Food Chem. 141, 1980–1986.
Elshafey, R., Tavares, A.C., Siaj, M., Zourob, M., 2013. Biosens. Bioelectron. 50, 143–149.
Elyasi, M., Khalilzadeh, M.A., Karimi-Maleh, H., 2013. Food Chem. 141, 4311–41317.
Evtugyn, G., Cherkina, U., Porfierva, A., Danzber, J., Ebner, A., Hianik, T., 2013. Electroanalysis 25, 1855–1863.
Hu, J., Zheng, P.-C., Jian, J.-H., Shen, G.-L., Yu, R.-Q., Liu, G.-K., 2009. Anal. Chem. 81, 87–93.
Jiang, Z., Yang, T., Lui, M., Hu, Y., Wang, J., 2014. Biosens. Bioelectron. 53, 340–345.
Karimi-Maleh, H., Biparva, P., Hatami, M., 2013. Biosens. Bioelectron. 48, 270–275.

Kaushik, A., Vasudev, A., Arya, S.K., Bhansali, S., 2013. Biosens. Bioelectron. 50, 35–41.
Kobrinsky, B., Karpatkin, S., 2009. In: Maragoudakis, M.E., Sopanoglou, N.E. (Eds.), Thrombin: Physiology and Disease. Springer, New York, pp. 161–172.
Latham, J.A., Johnson, R., Toole, J.J., Sciences, G., Drive, L., City, F., 1994. Nucleic Acid Res. 22, 2817–2822.
Li, L.-D., Zhao, H.-T., Chen, Z.-B., Mu, X.-J., Guo, L., 2011. Sens. Actuators B: Chem. 157, 189–194.
McClain, D.L., Woods, H.L., Oakley, M.G., 2001. J. Am. Chem. Soc. 123, 3151–3152.
Montrose, A., Cargou, S., Nepveu, F., Manczak, R., 2013. Biosens. Bioelectron. 49, 305–311.
Moradi, R., Sebt, S.A., Karimi-Maleh, H., Sadeghi, R., Karimi, F., Bahari, A., Arabi, H., 2013. Phys. Chem. Chem. Phys. 15, 5888–5897.
Niu, Y., Wang, P., Zhao, Y., Fan, A., 2013. The Analyst 138, 1475–1482.
Polverini, P.J., 1995. Crit. Rev. Oral Biol. Med. 6, 230–247.
Pui, T.S., Kongsuphol, P., Arya, S.K., Bansal, T., 2013. Sens. Actuators B: Chem. 181, 494–500.
Shainoff, J.R., Page, I.H., Andrasi, D., 1960. Circ. Res. 8, 1013–1022.
Shahmiri, M.R., Bahari, A., Karimi-Maleh, H., Hosseinzadeh, R., Nirnia, N., 2013. Sens. Actuators B: Chem. 177, 70–77.
Tsopanoglou, N.E., Maragoudakis, M.E., 2009. In: Maragoudakis, Micheal E., Tsopanoglou, N.E. (Eds.), Thrombin: Physiology and Disease. Springer, New York, pp. 93–114.
Wang, Y., Xiao, Y., Ma, X., Li, N., Yang, X., 2012. Chem. Commun. 48, 738–740.
Xu, H., Gorgy, K., Gondran, C., Le Goff, A., Spinelli, N., Lopez, C., Defrancq, E., Cosnier, S., 2013. Biosens. Bioelectron. 41, 90–95.